4. Observation of ice lensing and frost heaving (Exp. 1. 2)

When a porous medium consisting of water and fine particles, such as soil, is frozen unidirectionally, the water sometimes forms regions of ice that are almost devoid of particles. These regions are called ice lenses, and repetition of the process results in the formation of intermittent layers. The formation of ice lenses is recognized as a necessary condition for frost heave. In this case, there are some questions we must consider, that is, how the ice lens generates, grows and forms the layer, what are factors that mainly affect the ice lensing, and what kind of microstructure do ices make near freezing front. To clarify these questions, in this chapter, images of the samples in freezing process were directly observed by using unidirectional freezing apparatus equipped with microscope. Such experiment, which can observe formation of the intermittent layers in freezing sample continuously and microscopically, has not carried out except a few experiments.

4.1 Sample and method

Samples used here were the sample 1, 4 and 5. The sample 1 was mixed with distilled water to make slurry and deaired by a vacuum pump. The slurry was placed in an acrylic cylinder with 10-cm diameter and consolidated at an overburden pressure of 1 MPa for a week. A 3 mm-thick rectangular sample was obtained by cutting the consolidated sample. The samples 4 and 5 were mixed with distilled water and deaired by boiling. Water contents of prepared samples 1 and 4 were 46% and 80%, respectively. The samples 2-5 hardly have plastic condition. Consistency condition of these samples drastically change at their liquid limit. Then, two types of water contents were prepared for sample 5; one was the fluidized sample with water content

of 35% (sample 5s), and other was non-fluidized sample with water content of 33% (sample 5c). In this connection, we can say that the sample 4 was fluidized sample.

These prepared samples were placed into sample cell as shown in figure 14. The cell was composed of a pair of slide glasses (Matunami S-1111) and acrylic spacers. The cell had a capacity of 20.0 × 70.0 × 3.0 mm^3. Both sides of the cell were sealed with silicone to keep saturated condition, except for a small hole on one side to relieve pressure. The cell for the sample 1 and 5 had a water reservoir at the warmer side to supply water and had two pair of copper-constantan thermocouples with diameter of 0.2 mm, calibrated with an accuracy of 0.03 ˚C to measure temperature.

When different temperatures were given to each end of the sample cell, the isotherm advance in the sample until a steady state was attained. Then, we separated the experiment two stages. In the first stage (**Exp. 1**), we observed the vicinity of a growing ice lens immediately after temperature gradient was applied until the warmest ice lens almost stopped growing. The final temperature gradients α given to the cell are listed in Table 2. This kind of freezing would correspond to frost penetration in actual field in which freezing rate decreases gradually. In the second stage (**Exp. 2**), the cell was moved toward cold side at a constant rate of V_s after a temperature gradient was given to a sample cell for 1 hour. Since the advancing rate of the isotherm had decreased to enough low for 1 hour, the V_s gave a constant freezing rate V_f to the sample ($V_f = - V_s$). Then, we observed the vicinity of ice growing surface for duration until the cell was moved by 20-mm distance. The condition on the temperature gradient α at steady state, and sample moving rate V_s are listed in Table 2. Temperatures at two points, which were apart 4 mm and sandwiched the freezing front, were measured. Each temperature gradient was calculated from the temperatures. When the sample applied extremely rapid V_s, pore water would freeze there; i.e. ice lens could not form. Therefore, V_s were applied within the range which ice lens can form.

This kind of freezing can be regarded as frost heave under a constant freezing rate.

During each experiment, the apparatus was located in the ambient temperature of 5.0 ˚C, so that the initial temperature of the sample was 5.0 ˚C. Ice segregation and ice lens growth near the freezing front were observed with a microscope (40 magnification). The microscope was equipped with a charge coupled device (CCD) camera and a video system. Sample images were captured in one-minute interval. The sample images was divided with 20-μm mesh by a computer and the ice lens growth rate was measured from a relative coordinate of the growth surface. And the temperature of ice segregation was measured from the temperature profile that was traced on the image.

Table 2. Experimental conditions (**Exp. 1** and **Exp. 2**).

Sample		1,4,5	1	4	4
No.	Vs \ α	0.2	0.125	0.28	0.33
Exp.1	-	A0	B0	C0	D1
Exp.2	0.4	A1	B1	C1	D2
	0.6	A2	B2	C2	D3
	0.8	A3	B3	C3	D4

* V_s (μm/sec): α (˚C/mm)

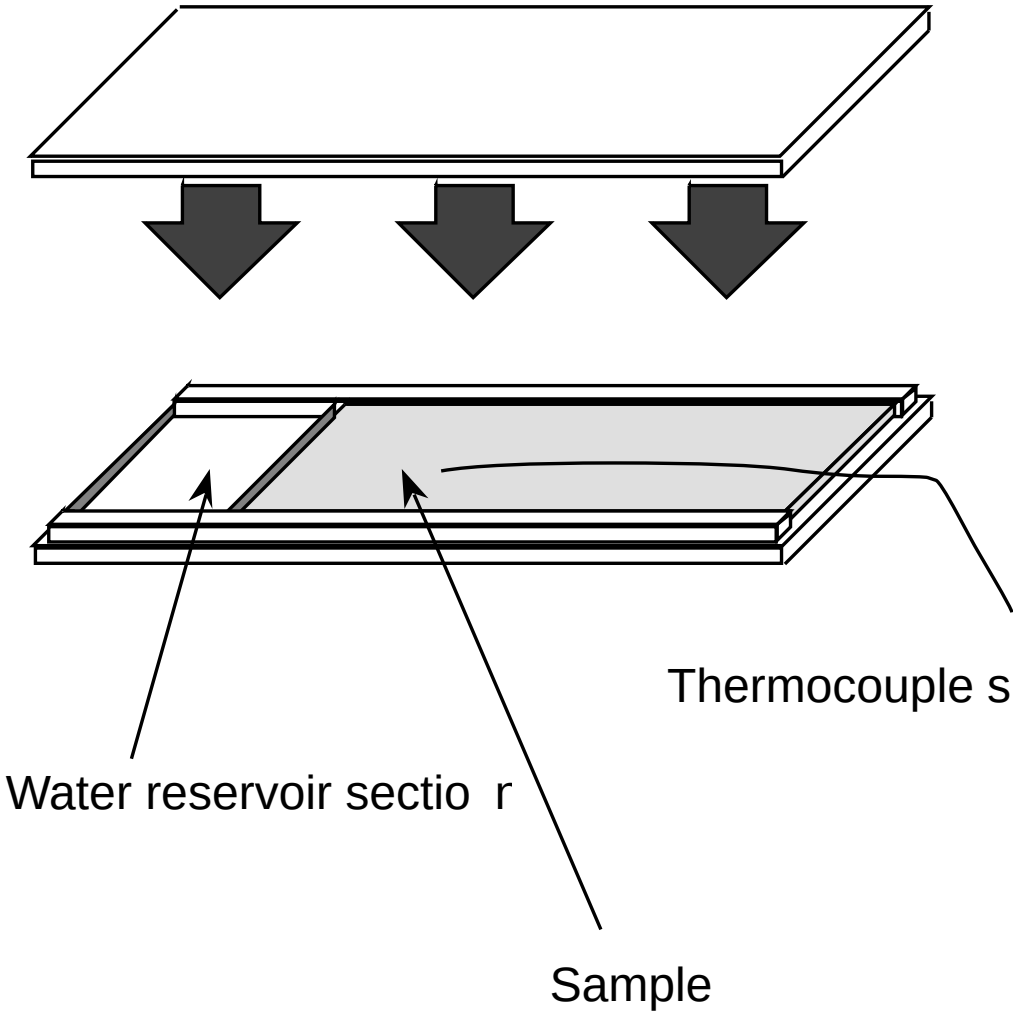

Fig. 14. Schematic diagram of sample cell for unidirectional freezing experiment.

4.2 Experimental results

4.2.1 Freezing experiment with zero sample rate (**Exp. 1**)

(1) Image of the sample in freezing process

Figure 15a shows the image of the freezing sample 1 (Fujinomori soil) under the condition of A0 (V_s = 0 μm/sec, α = 0.20 ˚C/mm). It was observed that ice lenses segregated from the cold side (from up to down in the figure) and formed intermittent layers. An ice lens was thicker as it was at warmer location. And it was also observed that the warmest ice lens formed at a point below 0 ˚C isotherm. Neither pore ice larger than 10 μm nor a displacement of soil particles due to pore ice formation was found in the region between the warmest ice lens and 0 ˚C isotherm. Under the condition of A0, the warmest ice lens started to segregate at -0.55 ˚C and grew 1.7 mm thick during time period of 400 minutes. The temperature at the growth surface of the warmest ice lens increased gradually and reached -0.2 ˚C.

Figure 15b shows the image of the freezing sample 4 (water saturated uniform size glass particles) under the condition of D0 (V_s = 0 μm/sec, α = 0.33 ˚C/mm). Black and white portions are ice lenses and glass particles, respectively. Ice lenses segregated from the cold side (from up to down in the figure) and formed intermittent layers, just same as in sample1. An ice lens was thicker as it formed later. Such ice lensing was observed in other experiments under different temperature gradients for V_s = 0 μm/sec. Under the condition of D0, the warmest ice lens grew to 3.5 mm thick for 10 hours. The growth surface of ice lenses in the sample 4 was flatter than in the sample 1. The ice lenses in the sample 4 made clearer layer in the perpendicular to heat flow than the ice lenses in the sample 1. And a boundary of ice lens observed in the sample 4 was much clearer than in the sample 1. These observations show that frost heave may occur in glass particles as well as in soil. Therefore, observing ideal ice lensing in the sample 4 will be useful to make ice lensing model.

Figure 15c shows the image of the freezing sample 5s (water saturated non-uniform size glass particles) under the conditions of A0 (V_s = 0 μm/sec, α = 0.20 ˚C/mm). The sample was freezing from up to down in the figure. Ice lensing was also observed in this sample as it as in other samples. Under the condition of A0, the warmest ice lens started to segregate at -0.37 ˚C and grew 1.4 mm thick during time period of 400 minutes. The temperature at the interface between the warmest ice lens and particles increased gradually and reached -0.08 ˚C. Comparing ice lens in sample 5 with that in the sample 1 and 4, ice lens in the sample 5s has medium roughness of the growth surface and clearness of the boundary. When an ice lens was growing, aggregated particles sometimes moved through the ice lens to warmer side. Such migration of aggregated particles in the sample 5s was similar to that in the sample 1 than that in the sample 4. It is suggested that the difference of uniformity of particle size and frame structure of particles affect to disturb shape of the ice lenses.

Here, we observed the growth of the warmest ice lens in each sample and measured the temperatures at growth surface observed in the samples 1 and 5.

(2) Thickness of the warmest ice lens

Figure 16a shows the change in thickness of the warmest ice lens in the sample 1 for specimens A0 and B0. Specimen A0 was frozen at a larger temperature gradient than specimen B0 (Table 2). The elapsed time was counted from start of segregation of the warmest ice lens. The ice lens grew rapidly in the beginning, and grew more slowly at later time stages. After 400 minutes, thicknesses of the ice lenses were 1.7 mm and 1.3 mm for A0 and B0, respectively. These results indicate that the thickness of ice lens increase more at the larger temperature gradient and that the growth of ice lens stabilized with time. The difference in the thickness of ice lens between A0 and B0 came from the difference in the growth rates in the early stages of the experiment.

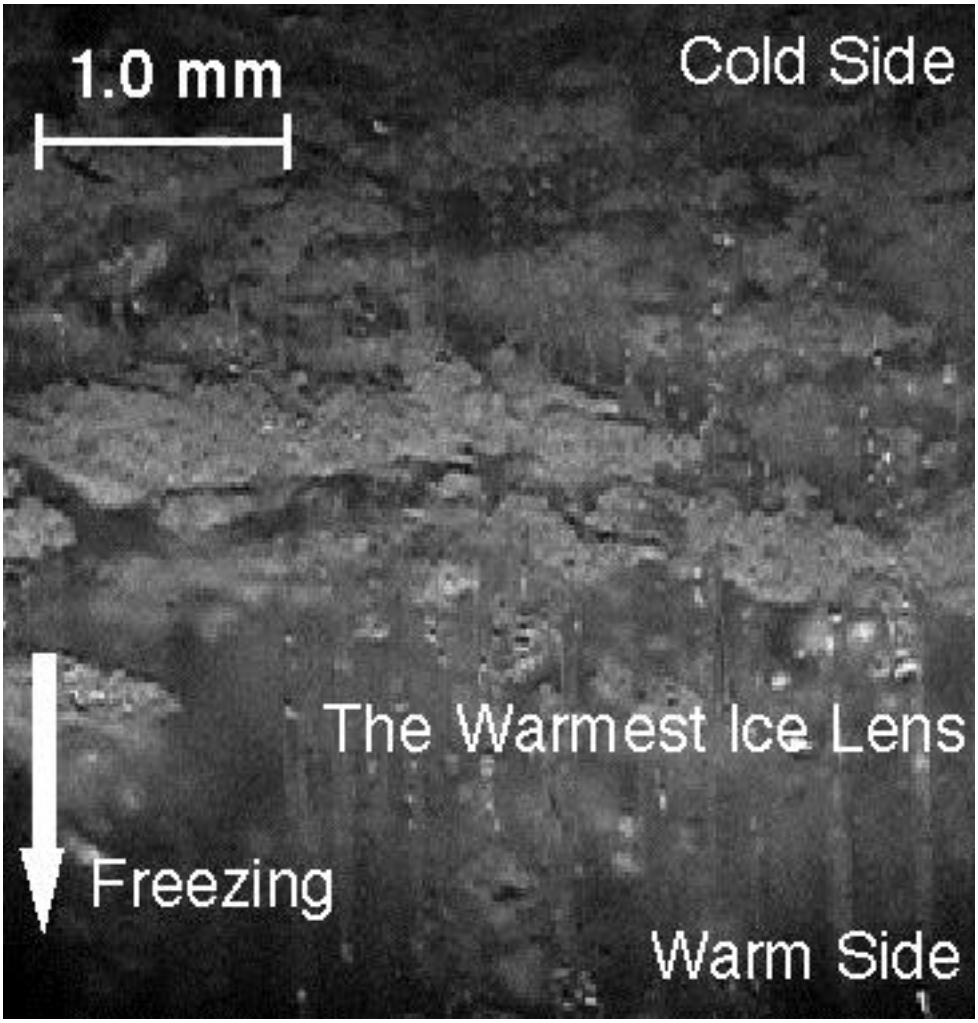

Fig. 15a. An image of the freezing sample 1 (Fujinomori soil) under the condition of A0 (V_s = 0 μm/sec, α = 0.20 ˚C/mm).

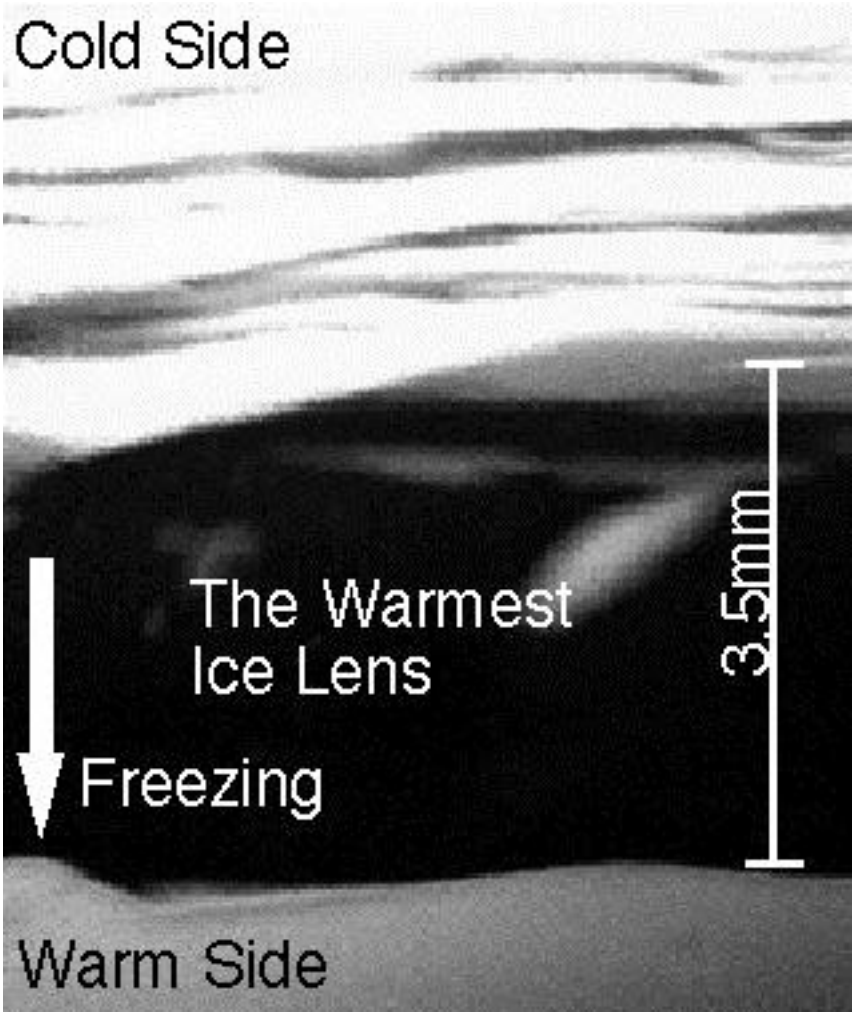

Fig. 15b. A image of the freezing sample 4 (glass particles) under the condition of D0 (V_s = 0 μm/sec, α = 0.33 ˚C/mm).

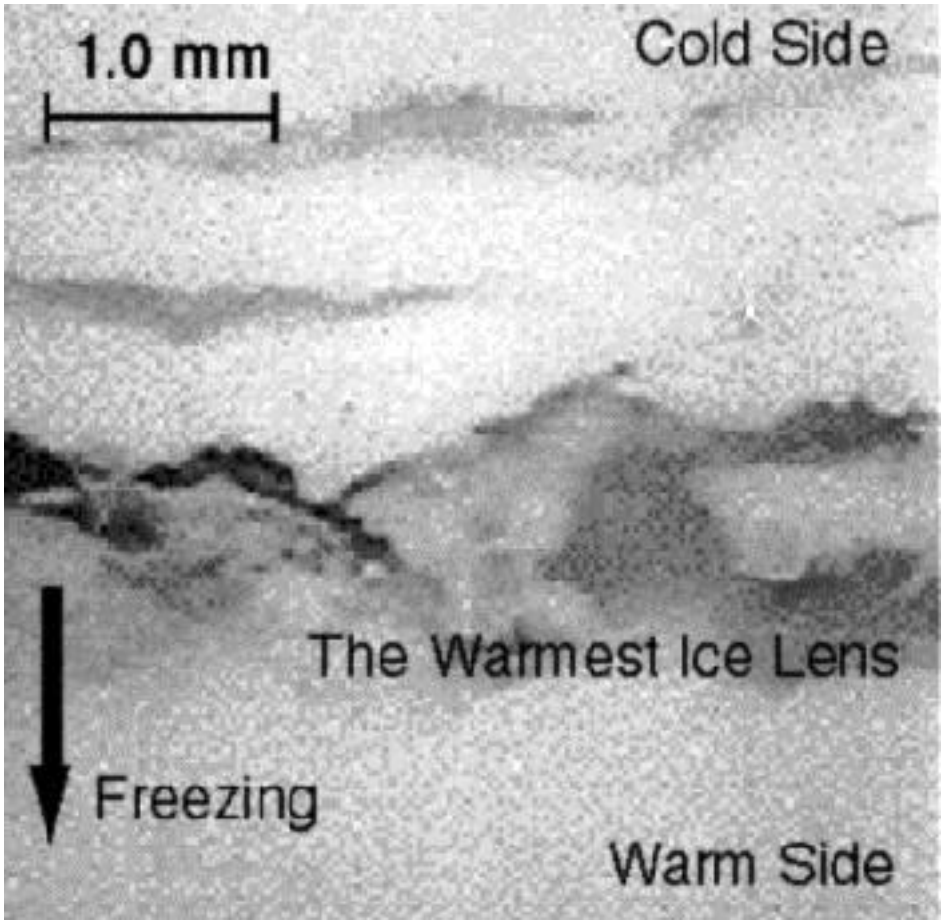

Fig. 15c. An image of the freezing sample 5s (water saturated non-uniform size glass particles) under the conditions of A0 (V_s = 0 μm/sec, α = 0.20 ˚C/mm).

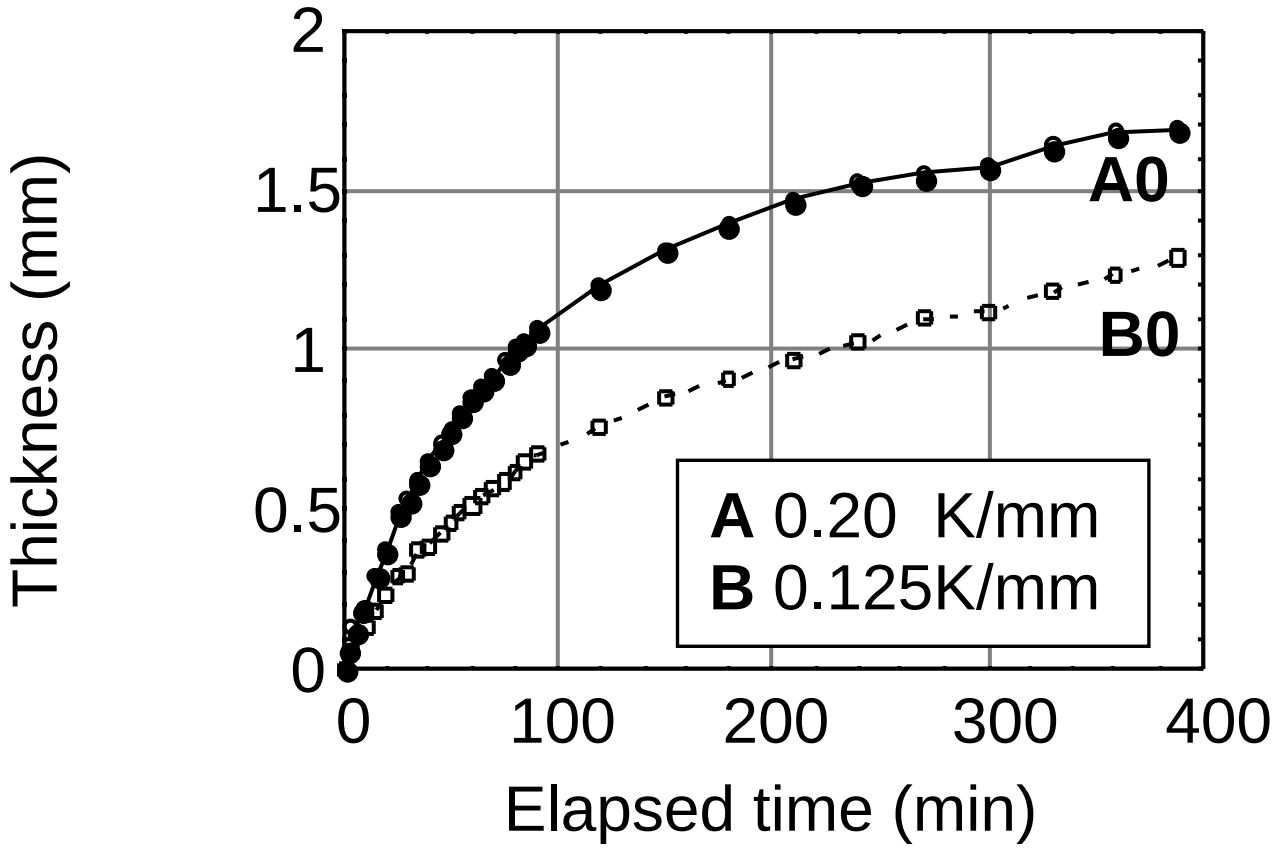

Fig. 16a. The change in thickness of the warmest ice lens in the sample 1 for specimens A0 and B0.

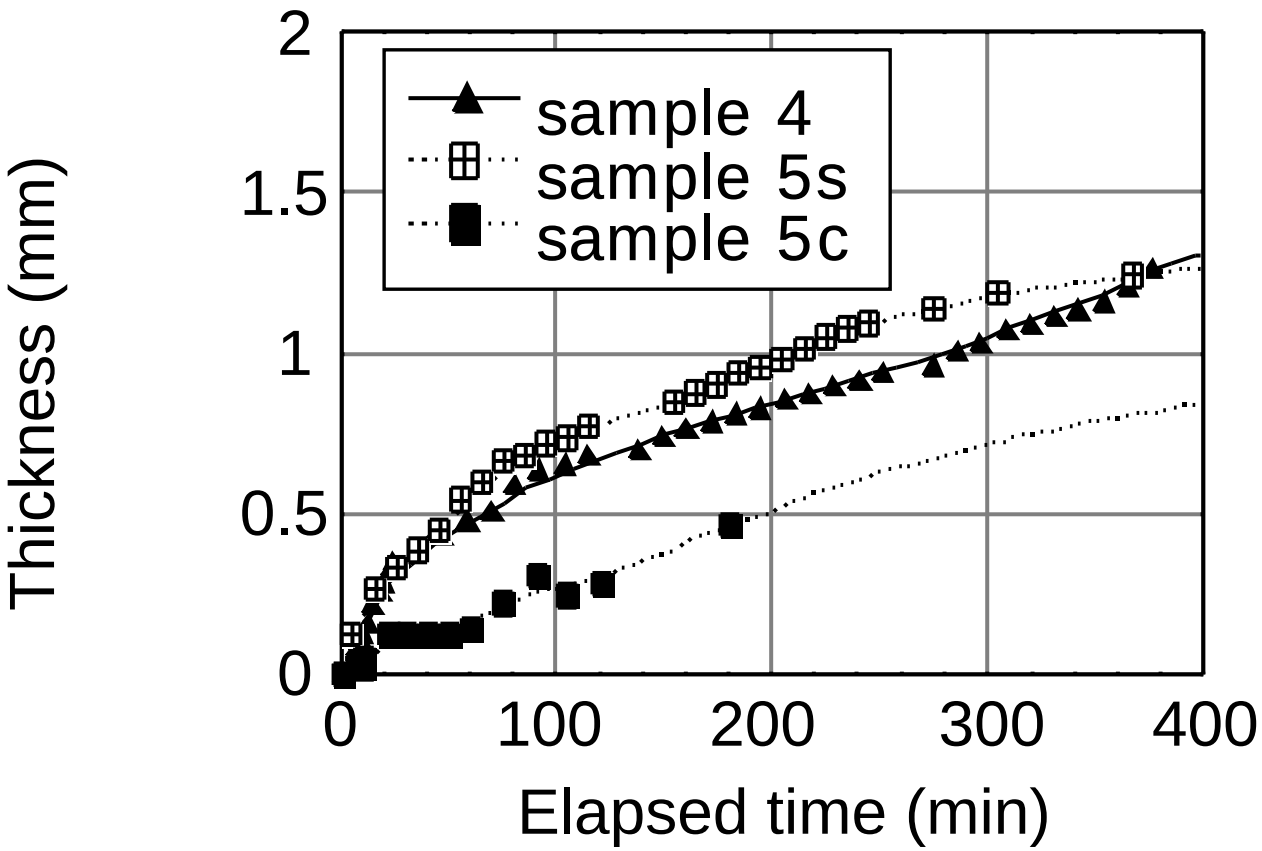

Fig. 16b. The change in thickness of the warmest ice lens in the samples 4, 5s and 5c.

Figure 16b shows the change in thickness of the warmest ice lens in the samples 4, 5s and 5c. The axes are same as in the figure 16a. All of the warmest ice lenses were grew rapidly in the beginnings, and grew more slowly at later time stages as it as in the sample 1. After 400 minutes, thicknesses of the warmest ice lenses were 1.4 mm, 1.4 mm and 0.8 mm for the samples 4, 5s and 5c. The thickness of the warmest ice lens in the sample 4 and 5s were thinner than in sample 1. And, fluidized sample (sample 5s) has thicker ice lens than non-fluidized sample (sample 5c). These results indicate that the thickness of ice lens will be changed by the slight difference of packing condition of particles and temperature condition than uniformity of particles.

(3) Temperature at growth surface of the warmest ice lens

Figure 17a shows temperatures at the growth surface of the warmest ice lens observed in sample 1. The temperatures increased with time and were gradually approaching -0.2 ˚C. The temperatures at which the warmest ice lenses started to form were -0.55 ˚C and -0.4 ˚C for A0 and B0, respectively. When the temperature gradient was steeper, the warmest ice lens started to form at a lower temperature. Figure 17b shows temperatures at the growth surface of the warmest ice lens observed in sample 5s under the condition of A0. The ice lens started to form and grew at warmer temperature than in sample 1.

Figure 18 shows growth rate of ice lenses observed in sample 1 as a function of temperature at the growth surface. The results in figure 18 were obtained from 7 experiments at conditions A0 and 3 experiments at conditions B0. No ice lenses grew at temperature above -0.21 ˚C. This figure indicates that the temperature at the growth surface determines the growth rate of ice lens. The best fit for the relationship between the growth rate of the ice lens V_{il} and the temperature is given by

$$V_{il} = 1.0\ \Delta T_{il}\ , \qquad (21)$$

where supper cooling degree ΔT_{il} is the temperature difference between the growth surface of ice lens and -0.21 ˚C.

Figure 19 shows growth rate of ice lenses observed in the sample 5 as a function of temperature at the growth surface. Supercooling degree ΔT_{il} for the sample 5 was the temperature difference between the growth surface of ice lens and -0.05 ˚C. The solid line is the best fit for sample 1 (equation 21). The relationship between growth rate and supercooling degree at the growth surface of the sample 5 was similar to the relation of the sample 1. These results indicate that not only the growth rate of the ice lens in sample 1 but also that in sample 2-5 can be expressed by same equation (21), if the supper cooling degree were accurately decided.

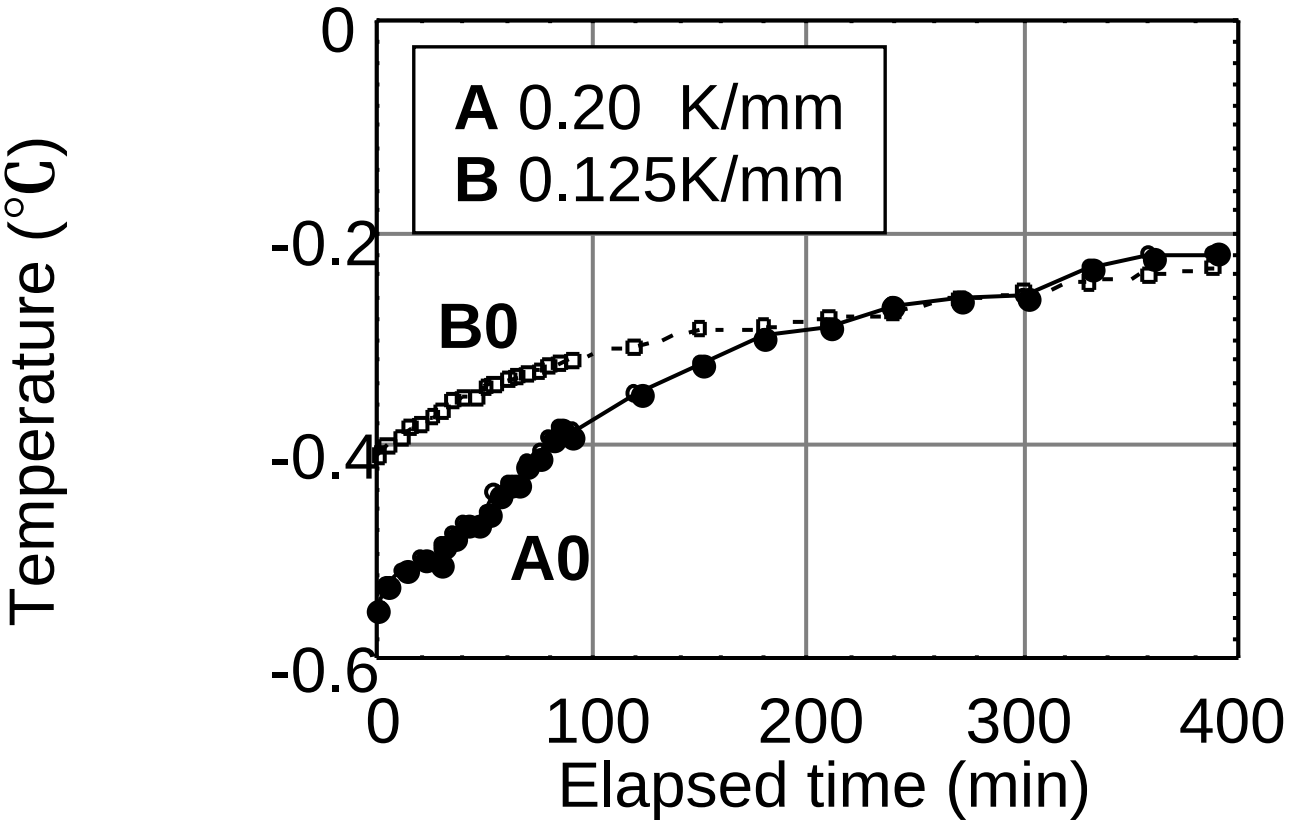

Fig. 17a. Temperatures at the growth surface of the warmest ice lens observed in sample 1.

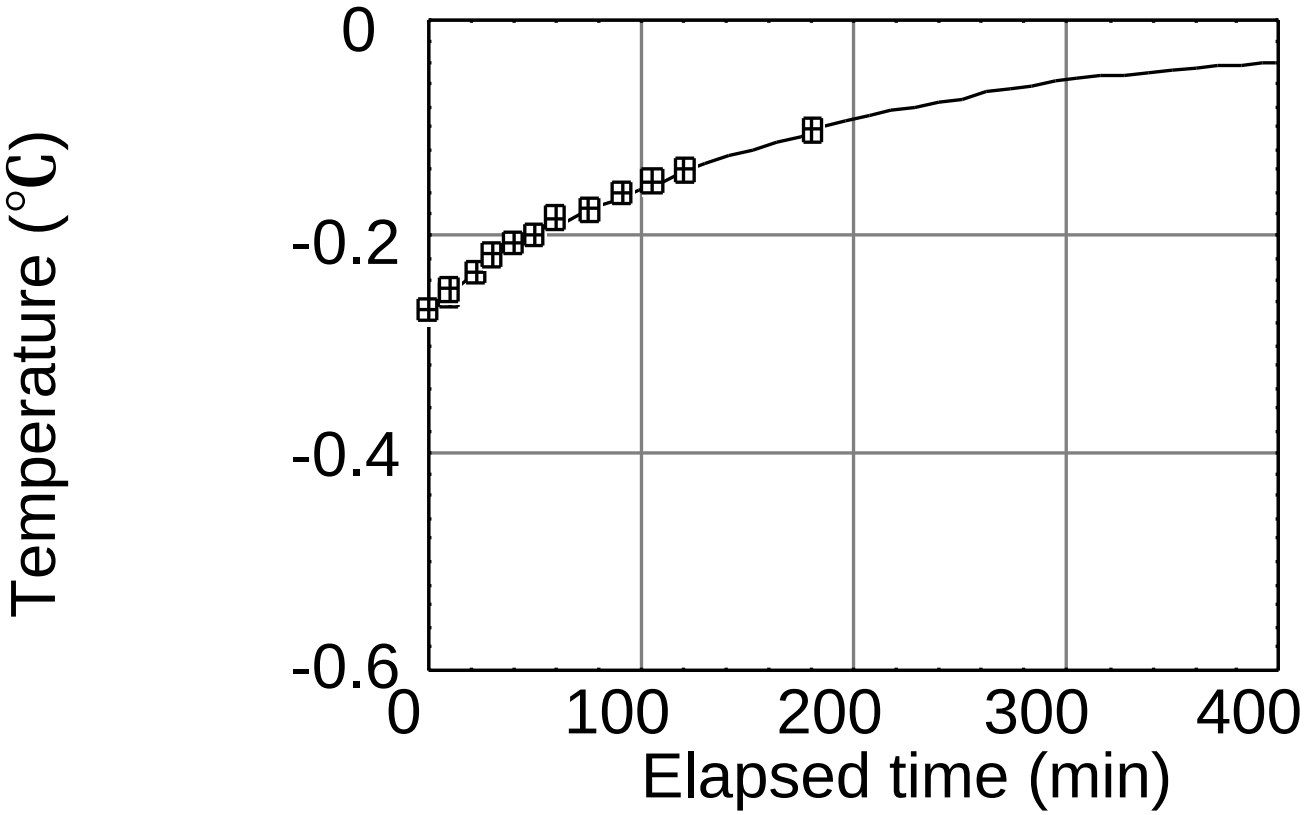

Fig. 17b. Temperatures at the growth surface of the warmest ice lens observed in sample 5s.

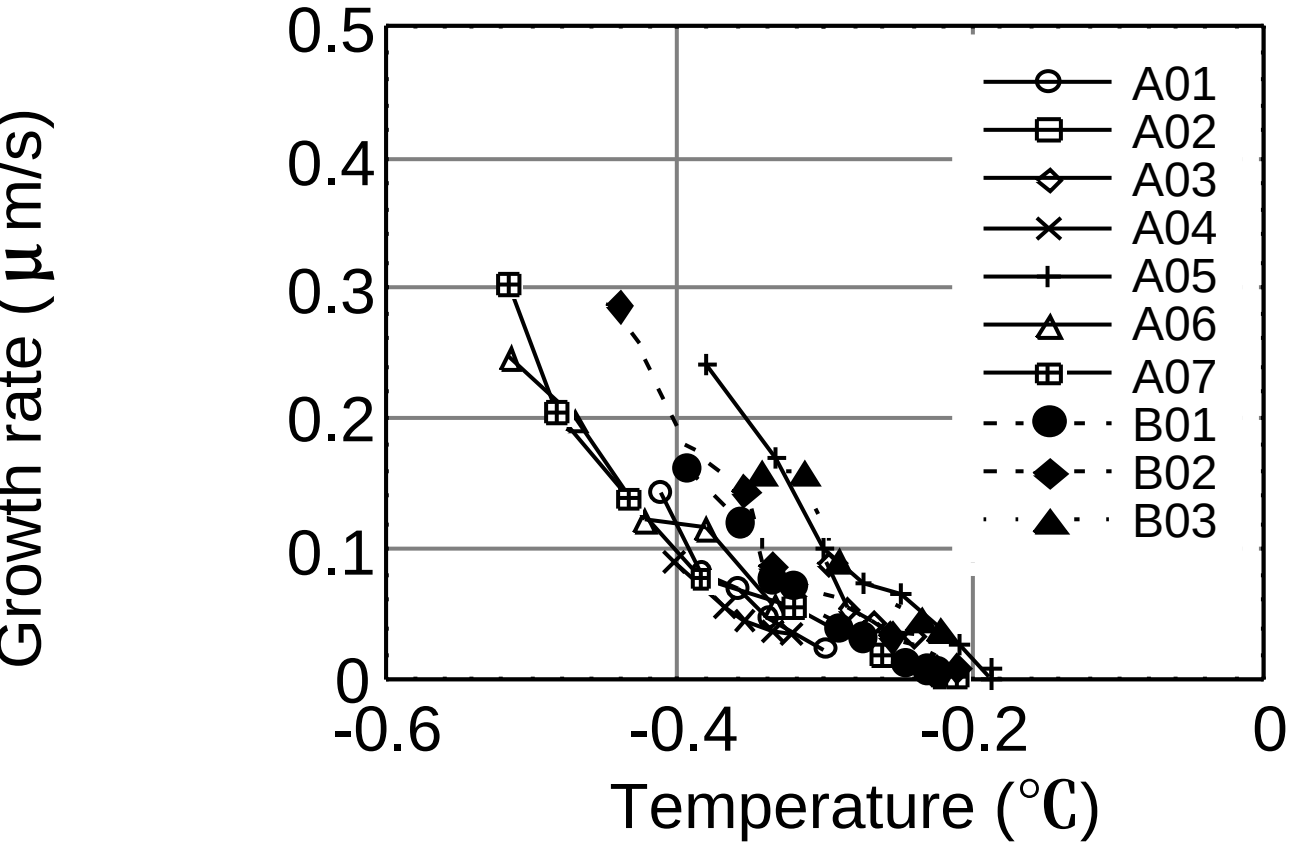

Fig 18. Relationship between growth rate of the warmest ice lens and temperature at the growth surface.

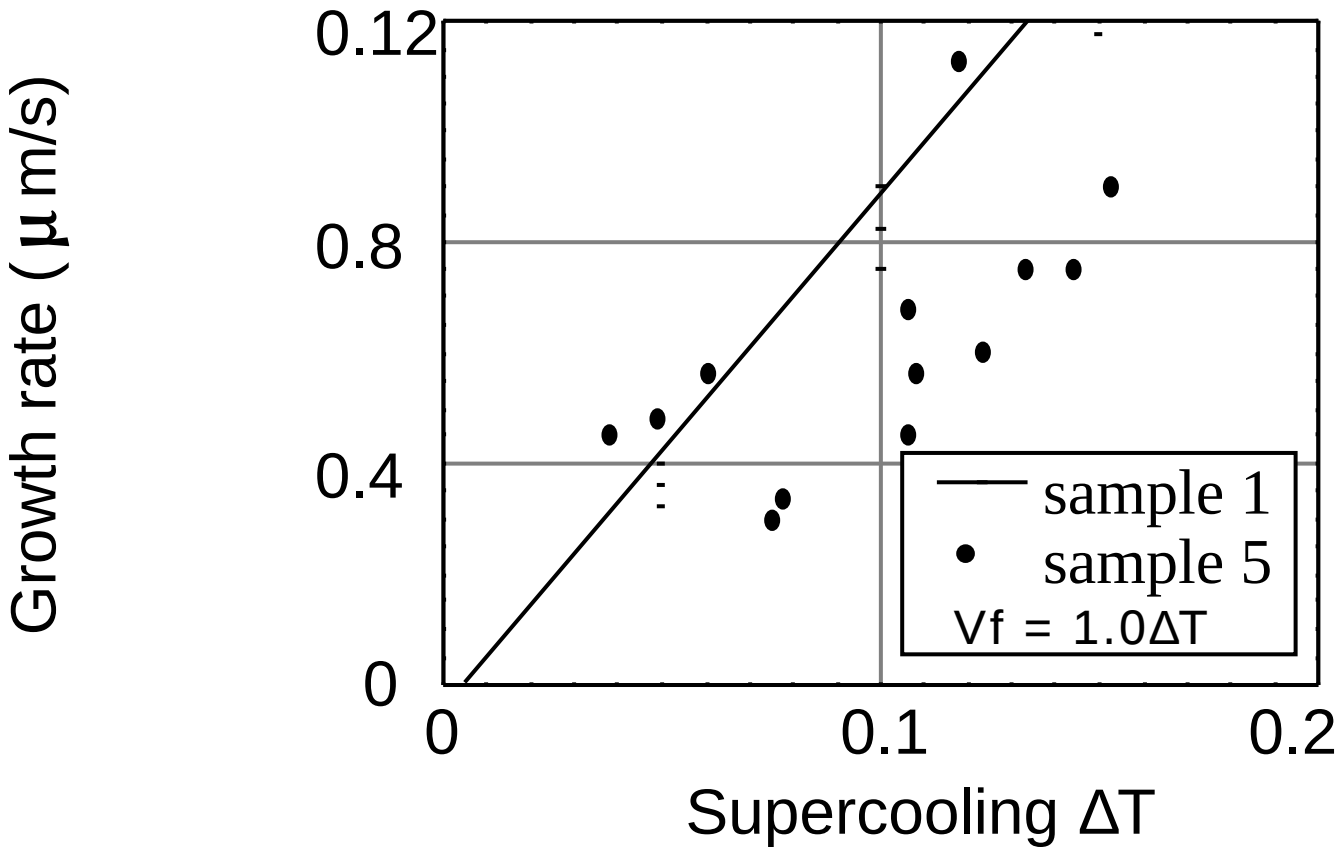

Fig. 19. Relationship between the growth rate of ice lens and supercooling degree at the growth surface.

4.2.2 Freezing experiment with constant sample rate (**Exp. 2**)

(1) Image of sample in freezing process

Figure 20a shows the image of freezing process for the sample 1 which was moving at constant rate of 0.60 μm/sec towards the frozen side with the temperature gradient of 0.2 ˚C/mm (A2). The sample was freezing from up to down in the figure. When the constant moving rate was applied, ice lenses rhythmically formed at the same location (at the same temperature) in the visual field of microscope. In this series of experiments, each ice lens was formed in a similar interval and had similar thickness. Once a new ice lens segregated on the warmer side, previously formed ice lenses stopped growing. This ice lens also stopped growing when a more recent ice lens started to segregate on the warmer side. In the case of A2, the segregation and the growth of ice lens were observed -0.5 ˚C.

Figure 20b shows the image of freezing process for the sample 4 under the condition of A3 (V_s = 0.80 μm/sec, α = 0.20 ˚C/mm). It was observed as it as in sample 1 that ice lenses with same thickness and same interval grew from cold side to warm side. The ice lens grew with pushing glass particles ahead at the growth surface. This growth surface moved toward cold side in the view field of microscope. This indicates that the growth rate of an ice lens was slower than V_f and that the temperature at the warmer end of the growing ice lens was lower than the temperature at which the ice lens started to grow. When the growth surface of ice lens moved by a distance from the location, at which the ice lens started to grow, the ice lens stopped growing and a new ice lens started to grow at the previous location. Figure 21 shows relationship between thickness of ice lens and sample moving rate. The thickness of ice lens decreased as the freezing rate increased.

Figure 20c shows the image of freezing process for the sample 5 under the condition of A2 (V_s = 0.60 μm/sec, α = 0.20 ˚C/mm). Stratified ice lenses rhythmically formed as it as in other samples. Although thickness and interval of ice lens observed in sample 4 were almost constant, they were in mess in the sample 4, sample 5 and sample 1 in that order. Figure 22 shows relationship between mean interval of ice lens and sample moving rate. The mean interval of ice lens decreased as the freezing rate increased. And the mean interval in the sample 5 was between that in the samples 1 and 4.

Here, we measured the total heave amount and occurring temperature of ice lens observed in sample 1.

(2) Total heave amount

Figure 23 shows total heave as a function of time for different sample moving rates. When sample was freezing, volume of the sample would be expanding. This expanded volume was called total heave. And it almost equals to the sum of thickness of all ice lenses in the sample. The total heave was determined by measuring movement of a soil particle on the images. In this series, the elapsed time was counted from the start of the sample cell movement. Total heave increased linearly with time for each specimen. The total heave increased with increasing freezing rate. Figure 24 shows relationship between heaving rate V_h and sample moving rate V_s. The solid line is the best fit for the experimental values for series A (α = 0.20 ˚C/mm) and the dashed line is for series B (a = 0.125 ˚C/mm). Heaving rate was about 60% of the moving rate.

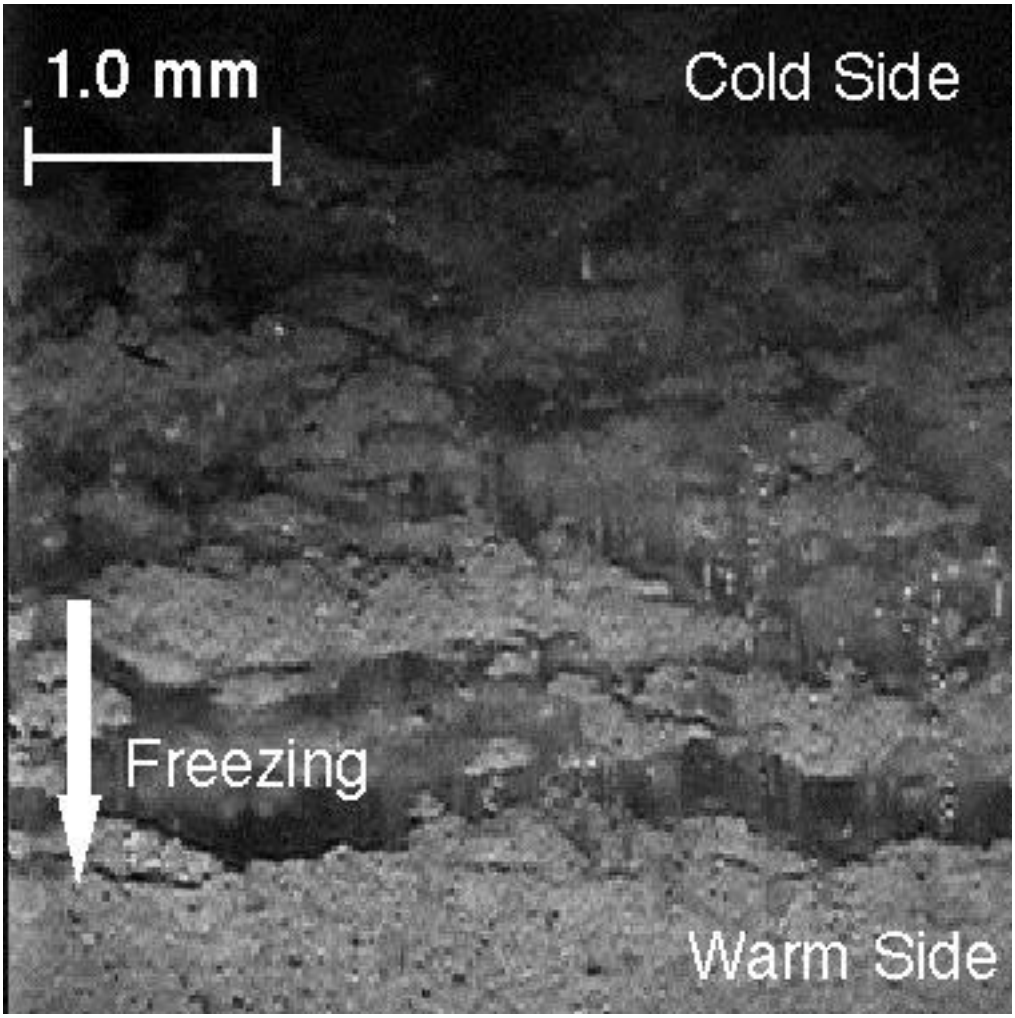

Fig. 20a. An image of the freezing sample 1 (Fujinomori soil) under the condition of A2 (V_s = 0.6 μm/sec, α = 0.20 ˚C/mm).

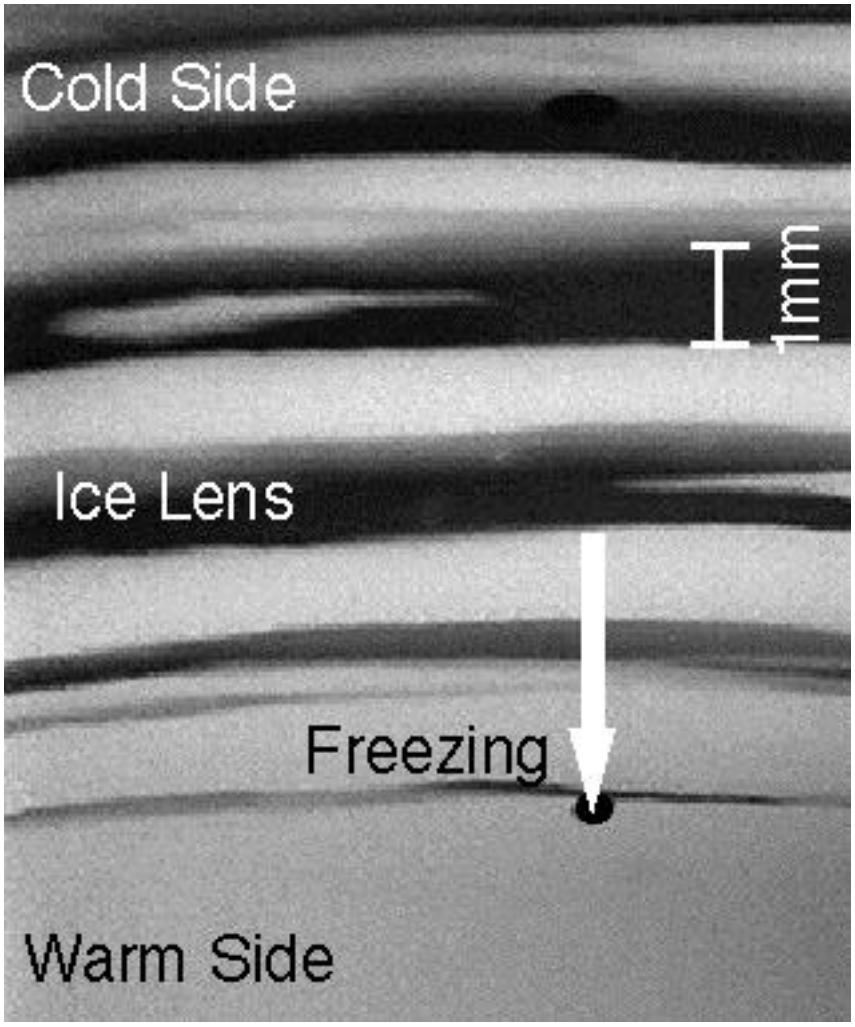

Fig. 20b. An image of the freezing sample 4 (glass particles) under the condition of D2 (V_s = 0.8 μm/sec, α = 0.20 ˚C/mm).

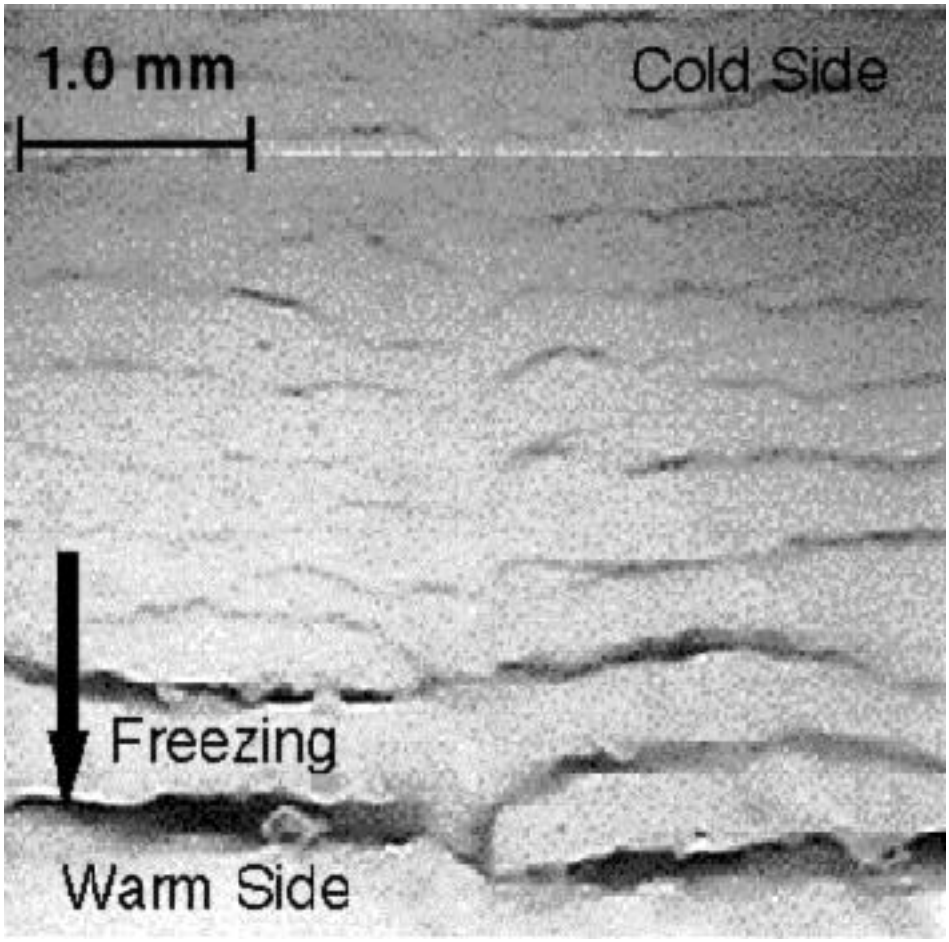

Fig. 20c. An image of the freezing sample 5s (water saturated non-uniform size glass particles) under the conditions of A2 (V_s = 0.6 μm/sec, α = 0.20 ˚C/mm).

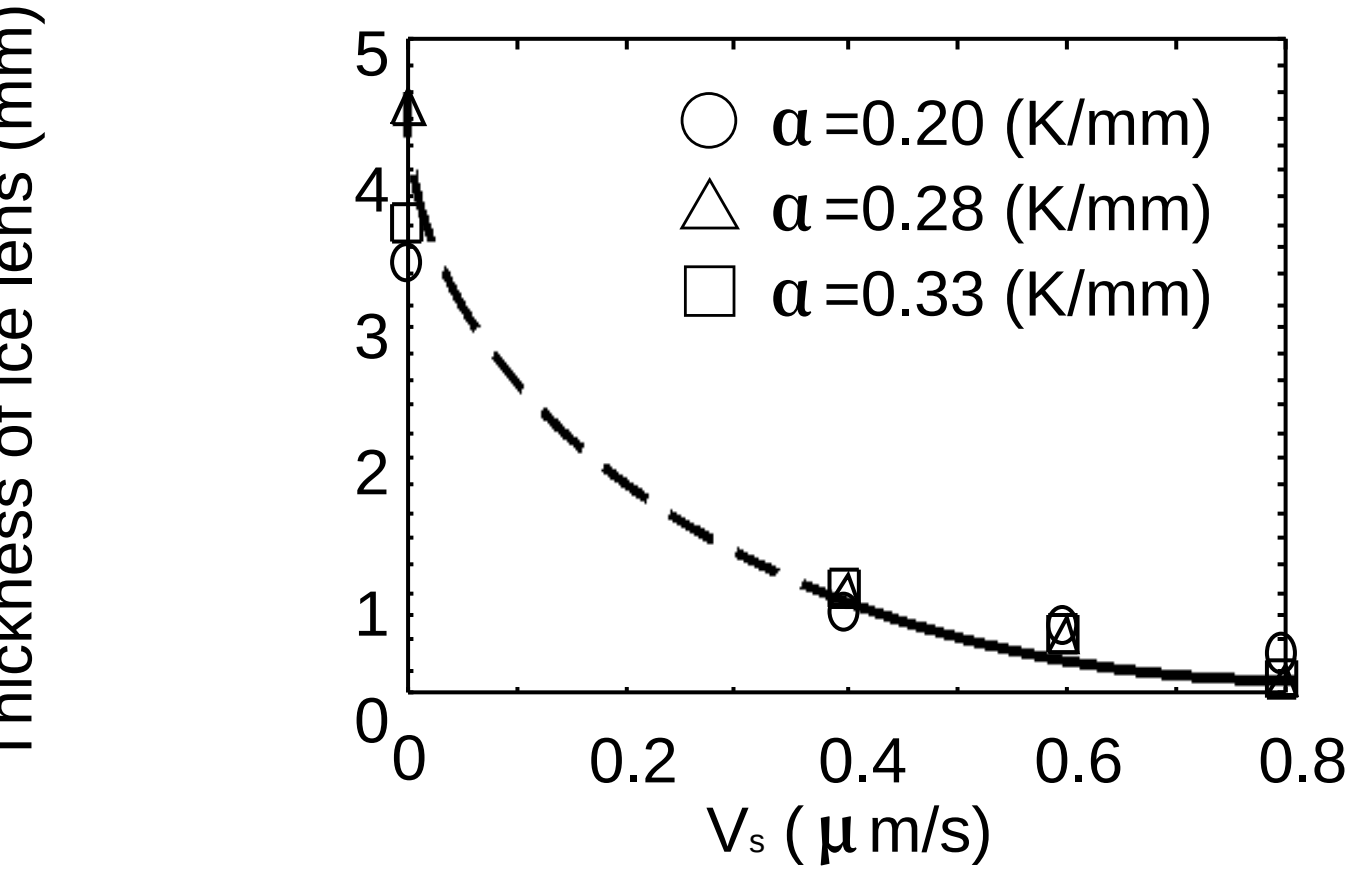

Fig. 21. Relationship between freezing rate and thickness of ice lens.

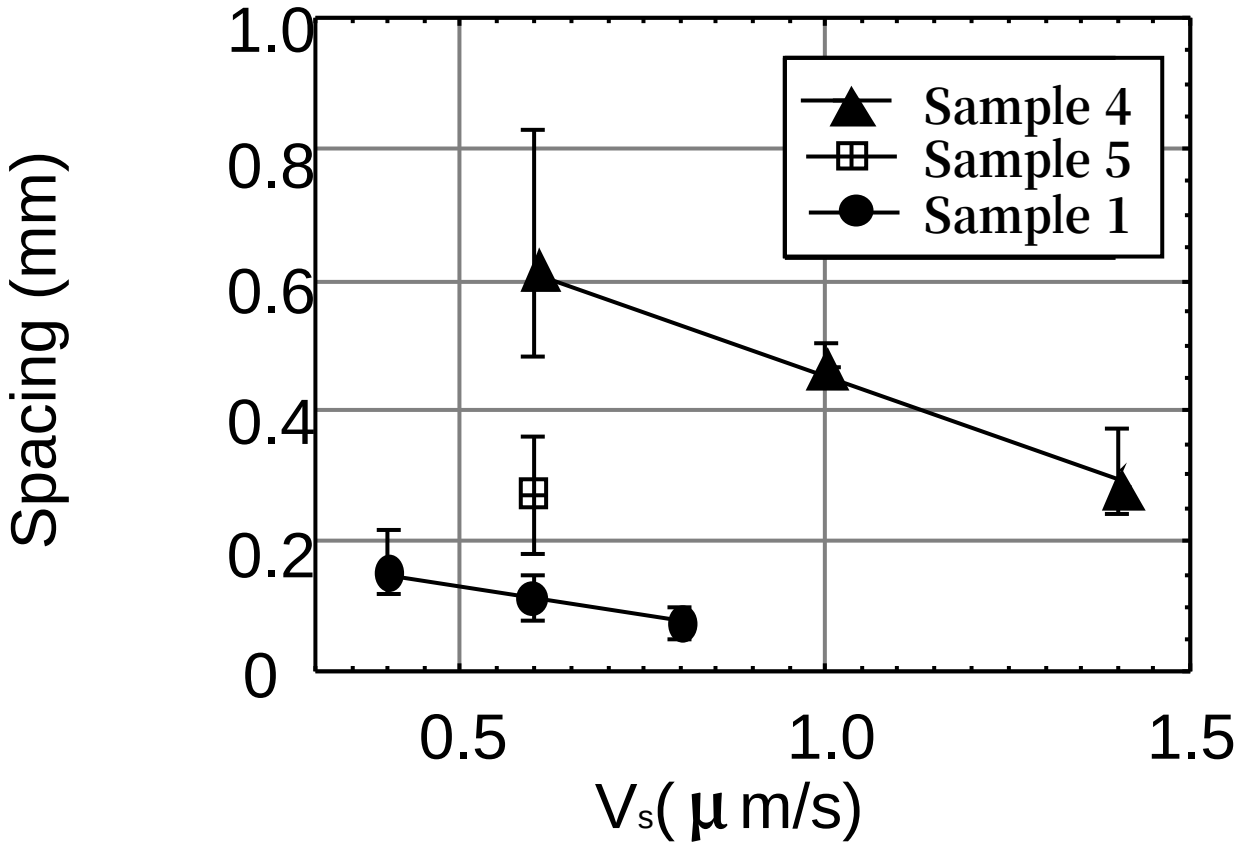

Fig. 22. Relationship between freezing rate and spacing between ice lenses.

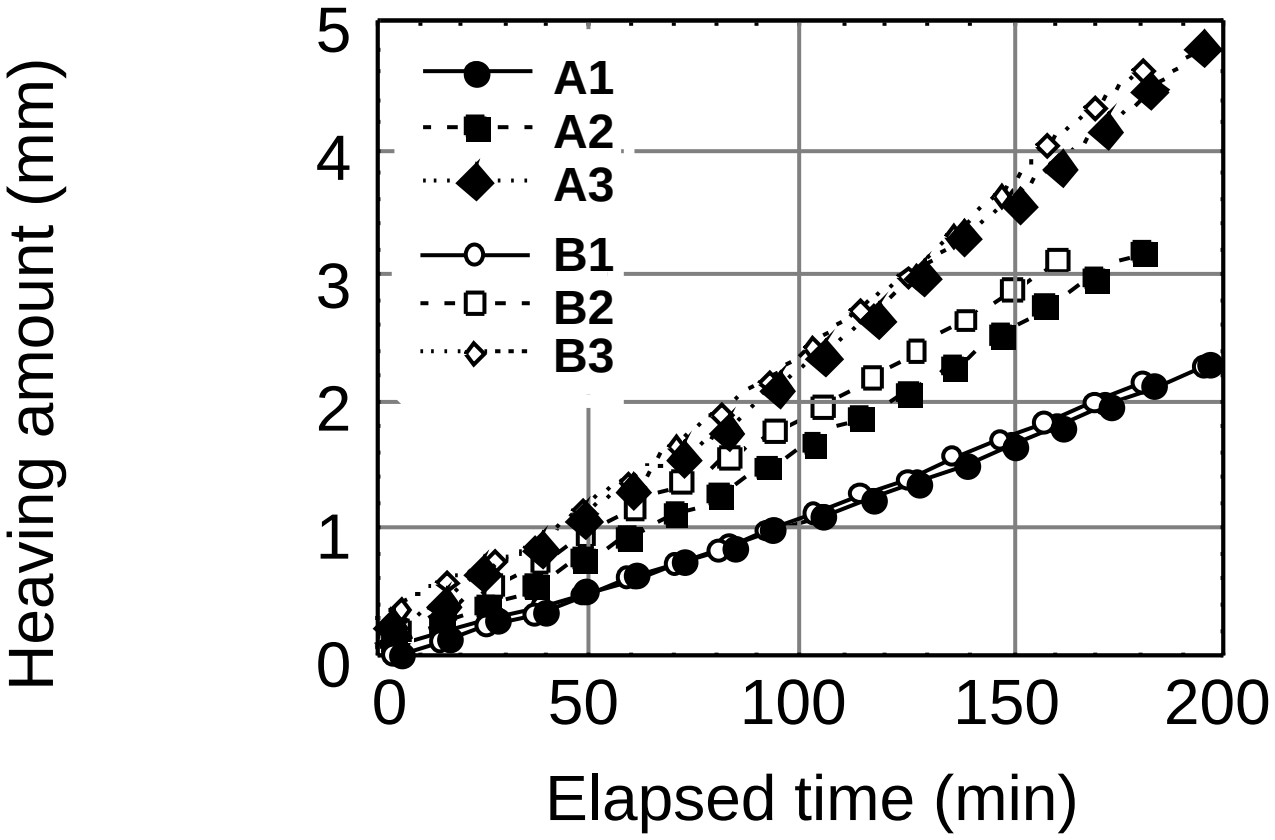

Fig. 23. Total heaving amount when a sample was moving with constant rate (sample 1).

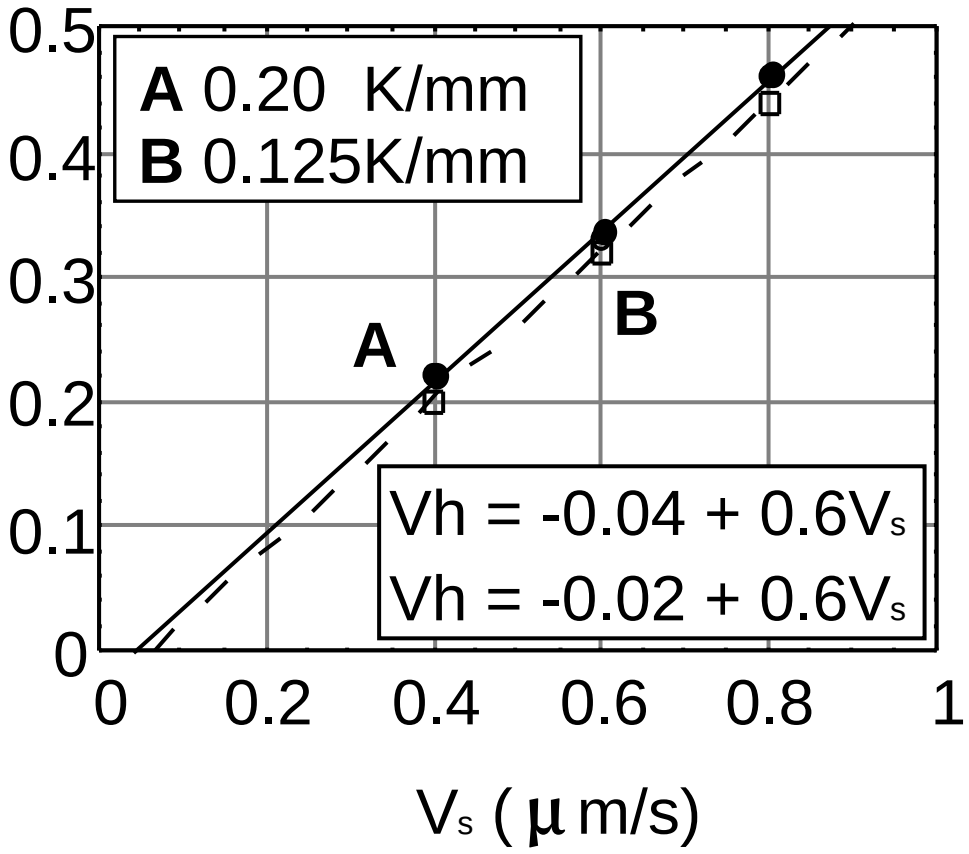

Fig. 24. Relationship between heaving rate and sample moving rate.

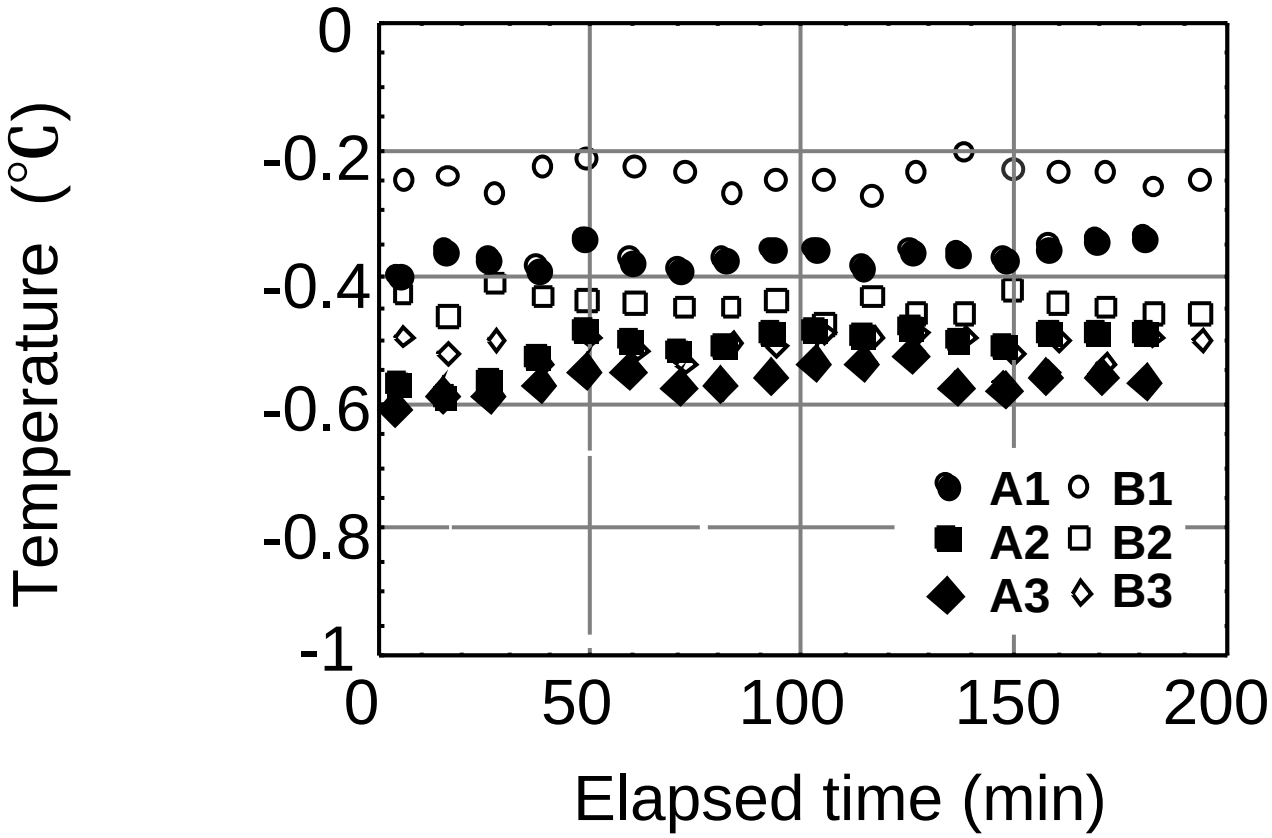

Fig. 25. Temperature at growth surface of ice lenses.

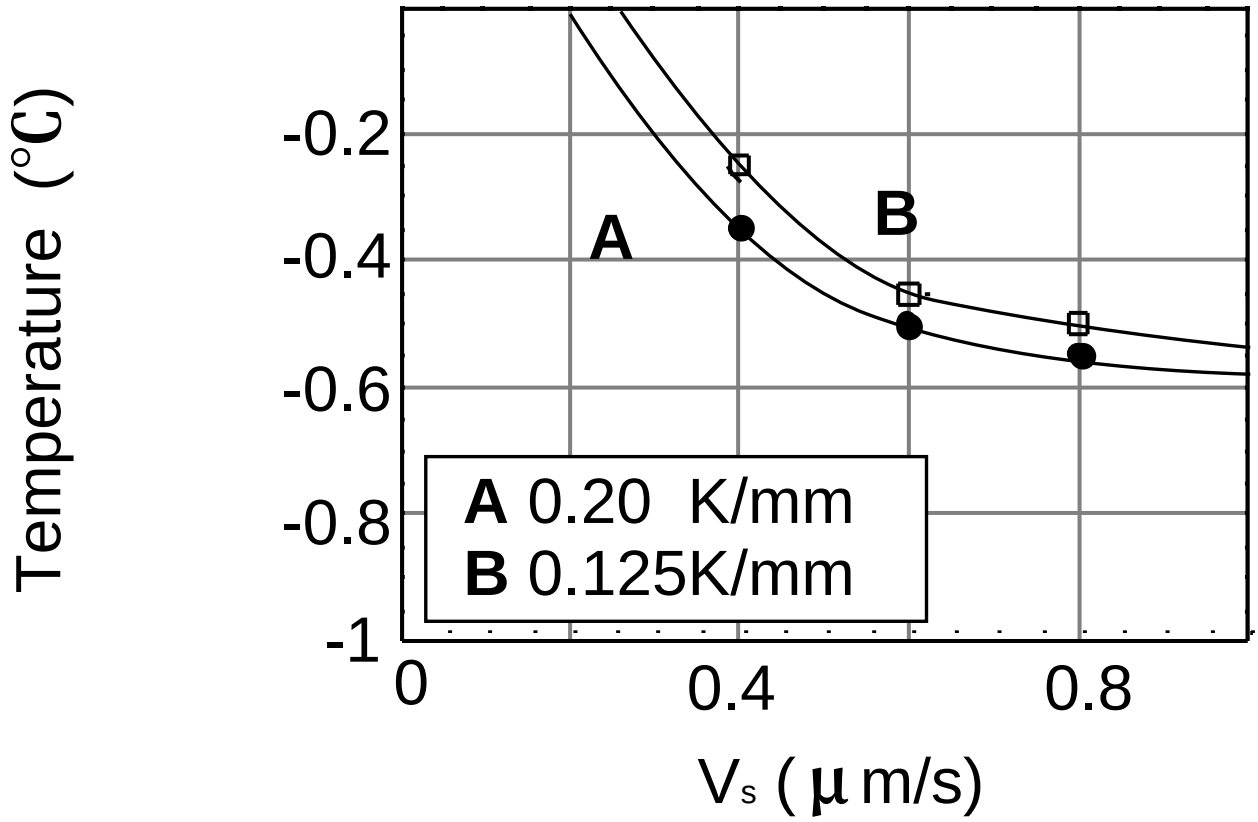

Fig. 26. Relationship between freezing rate and ice lens generation.

(3) Temperature at growth surface of ice lens

Figure 25 shows the segregation temperature for the ice lenses. The segregation temperature was defined as the temperature of the interface at which an ice lens started to grow. Each ice lens started to segregate at a constant temperature. Figure 26 shows relationship between the occurring temperature and the freezing rate. When the freezing rate and the temperature gradient were high, ice lens segregated at a lower temperature. This figure also indicate that the segregation temperature was dependent on the freezing rate than the temperature gradient

4.3 Discussion

We will discuss here a frost heave model by using the experimental results of this chapter. At first, we examine the frost heave model based on a partially frozen zone, so called frozen fringe.

In the frozen fringe model, frost heave is determined by the coupled of heat and water flow in the frozen fringe (e.g. Miller, 1980; Gilpin, 1980). It was assumed that soil water would flow through the frozen fringe with hydraulic conductivity K from the unfrozen zone to the growth surface of the ice lenses due to the pressure gradient dP/dx. If all water flowing to ice lens contributes to the warmest ice lens growth, the heave rate V_h is given by

$$V_h = - \frac{K}{\rho_w g} \frac{dp}{dx} \quad , \tag{22}$$

where ρ_i is the density of ice and g is the gravitational constant. Gilpin (1980) and Nixon (1991) have assumed that pore ice would grow so that unfrozen water content would decrease. They have expressed the hydraulic conductivity of the frozen fringe K as a function of temperature:

$$K = \frac{K_0}{(-T)^{\beta}} \quad , \tag{23}$$

where K_0 is the hydraulic conductivity of frozen sample at –1 ˚C, T is the temperature in the frozen fringe and β is an empirical constant. Equation (23) means that the hydraulic conductivity of the frozen fringe decreases exponentially with decreasing temperature of the frozen fringe. Consequently, the growth rate of the warmest ice lens calculated by equation (22) should decrease.

In our experiment, the growth rate of the warmest ice lens decreased with increasing temperature at the growth surface of ice lens as equation (21). The experimental result corresponds to not the frozen fringe model by Gilpin and Nixon but the experimental results by Vignes and Dijkema (1974), Biermans *et al*. (1978), Ishizaki *et al*. (1985) and Ozawa and Kinosita (1989). This discrepancy may come from the postulation that there would exist pore ice in the frozen fringe. Actually, no pore ice, which can change the hydraulic conductivity, larger than 10 μm can be observed (e.g. figure. 15 and figure. 20). And another experiment, which we performed by using electric resistibility, also find no pore ice in the zone between the warmest ice lens and 0 ˚C isotherm (Watanabe and Ishizaki, 1995).

If we assume that there is no pore ice in the frozen fringe, the frozen fringe has a constant hydraulic conductivity and the soil water flows to the surface of growing ice lens through the frozen fringe due to a temperature difference. By applying generalized Clausius-Clapeyron equation, pressure of the soil water on the growth surface of ice lens (MPa) is given by

$$\Delta p_w = 1.23\Delta(T_{il}-T_m)+0.11\,\Delta p_i + \Pi \quad , \tag{24}$$

where ΔP_w is the pressure difference between the soil water on the growth surface of ice

lens and an atmosphere, T_{il} is the temperature at the growth surface and T_m is the melting point of ice at an atmospheric pressure, ΔP_i is the pressure difference between ice lens and the atmosphere, and Π is the osmotic pressure of the soil water (Mizoguchi, 1993). For soil freezing without overburden pressure, ice pressure in the soil may be at the atmospheric pressure. In addition, the osmotic pressure may be negligible for salt free soil. Then equation (24) becomes

$$\Delta p_w = 1.23\Delta(T_{il}-T_m) \quad , \tag{25}$$

This equation means that the pressure difference can be expressed as a linear function of the temperature at the growth surface of ice lens. If it is assumed that the hydraulic conductivity of the frozen fringe and kinetic coefficient at the growth surface of ice lens are constant, the calculated ice lens growth rate would increase with decreasing the temperature at the growth surface of ice lens. This relationship between the growth rate and the temperature is consistent with our experimental results in equation (21). Nevertheless the ratio calculated from equation (25) is one order larger than our experimental result. To explain the difference between the calculation and the experimental results without considering frozen fringe, two possibilities can be considered. One is that an unfrozen water film on the growth surface of ice lens would have some kinetic resistance to supply water into ice crystal (surface kinetic effect), and the other is that crystallization temperature of ice would be changed by particles' condition near the growth surface (structural supper cooling). For the discussion of the kinetic process and supercooling in frost heave, however, more studies will be needed considering non-equilibrium process. In any possibility, our experimental results indicate that the growth rate of ice is determined by the kinetic process at the growth surface rather than the hydraulic conductivity in partially frozen zone (frozen fringe).

4.4 Summary

In this chapter, ice lensing and microstructure near freezing front was observed directly by using the unidirectional freezing apparatus. It was shown that ideal ice lenses for modeling can be made using uniform size glass particles. From the experiments, the following results were obtained. (1) No pore ice larger than 10 μm was formed in the frozen fringe. (2) The growth amount of ice lens would increase when the freezing rate and the temperature gradient were high. In this time, it was dependent on the freezing rate than the temperature gradient. (3) The growth rate of ice lens depended on the temperature at their growth surface. (4) The temperature of ice lens, which started to segregate, depended on the freezing rate. In addition, it was also suggested that the packing condition of particles near the ice growing surface affect to ice lensing, especially to the intervals and shapes.

It was concluded that freezing rate, supercooling degree at growth surface of the ice lens and particle condition near growing ice lens were important factors for the ice lensing mechanism.